

Article

Effect of Direct-Contact Ultrasonic and Far Infrared Combined Drying on the Drying Characteristics and Quality of Ginger

Zhenhua Feng^{1,2}, Minmin Zhang^{1,2}, Lanping Guo³, Rencai Shao⁴, Xiao Wang^{1,2}  and Feng Liu^{1,2,*}

- ¹ Key Laboratory for Applied Technology of Sophisticated Analytical Instruments of Shandong Province, Shandong Analysis and Test Center, Qilu University of Technology (Shandong Academy of Sciences), Jinan 250014, China; a3945fzh@163.com (Z.F.); zhangminminff@163.com (M.Z.); wangx@sdas.org (X.W.)
- ² Key Laboratory for Natural Active Pharmaceutical Constituents Research in Universities of Shandong Province, School of Pharmaceutical Sciences, Qilu University of Technology (Shandong Academy of Sciences), Jinan 250014, China
- ³ Resource Center of Chinese Materia Medica, State Key Laboratory Breeding Base of Dao-di Herbs, China Academy of Chinese Medical Sciences, Beijing 100700, China; glp01@126.com
- ⁴ Ningbo Scientz Biotechnology Co., Ltd., Ningbo 315100, China; 15275156220@139.com
- * Correspondence: liufeng8109@qlu.edu.cn

Abstract: In this study, the effects of ultrasonic power, drying temperature, and slice thickness on the drying rate, chromatism, water migration law, gingerol content, flavor, and antioxidant activity of ginger were investigated by using a direct-contact ultrasound and far infrared combined drying technology. The results showed that compared with single far infrared drying, direct-contact ultrasound and far infrared combined drying accelerated the free water migration rate of ginger (7.1~38.1%), shortened the drying time (from 280 min to 160 min), reduced the loss of volatile components in ginger, and significantly increased the antioxidant activity of ginger ($p < 0.05$). Furthermore, after ultrasound intervention, the gingerol content decreased in slices of 4 mm thickness (0.1226 ± 0.0189 mg/g to 0.1177 ± 0.0837 mg/g) but increased in slices of 6 mm thickness (0.1104 ± 0.0162 mg/g to 0.1268 ± 0.0112 mg/g). This drying technology has a certain reference significance for the drying process of ginger slices.

Keywords: ginger; drying; direct-contact ultrasound; infrared; flavor; quality



Citation: Feng, Z.; Zhang, M.; Guo, L.; Shao, R.; Wang, X.; Liu, F. Effect of Direct-Contact Ultrasonic and Far Infrared Combined Drying on the Drying Characteristics and Quality of Ginger. *Processes* **2024**, *12*, 98. <https://doi.org/10.3390/pr12010098>

Academic Editors: César Ozuna, Sueli Rodrigues and Fabiano André Narciso Fernandes

Received: 4 December 2023

Revised: 26 December 2023

Accepted: 27 December 2023

Published: 1 January 2024



Copyright: © 2024 by the authors. Licensee MDPI, Basel, Switzerland. This article is an open access article distributed under the terms and conditions of the Creative Commons Attribution (CC BY) license (<https://creativecommons.org/licenses/by/4.0/>).

1. Introduction

Ginger (*Zingiber officinale* Roscoe) is the fresh rhizome of Zingiberaceae perennial herb ginger [1]. It is a traditional spice and food seasoning and also a kind of traditional Chinese medicine with high medicinal value [2,3]. As a traditional Chinese medicine, it has the effect of relieving colds, vomiting, and coughs; warming the lungs; and detoxifying the body [4]. It is commonly used to treat wind chills, spleen and stomach illness, vomiting, lung cough and colds, and fish and crab poison [5]. Ginger contains a variety of bioactive substances, including gingerol, zingerone ginger oil, active polysaccharides, and glycoproteins [6,7]. However, due to the relatively high moisture in ginger, it is easily affected by environmental factors during storage and, thus, rotting. In order to improve the practical value of ginger, it is necessary to dry and process it. On the one hand, the drying process can reduce the moisture content of the sample and increase the sample storage time [8]. On the other hand, the relevant enzyme activity in the sample will also be effectively maintained [9], and the flavor was also improved in the samples after drying [10].

Although traditional drying methods (including sun exposure and air circulation) are simple and easy to use, excessive drying time can lead to excessive loss of volatile components in the sample, affecting the sample flavor and this drying method is easily limited by environmental conditions [11,12]. Therefore, it is necessary to develop new drying methods to improve the drying quality of ginger slices. Compared with ordinary

sun drying, the solar drying method not only shortened the drying time of samples but also retained the content of essential oil [13]. Also, this drying method is limited by climate. In recent years, new drying technologies have been widely used in the field of agricultural and by-product processing. Vacuum microwave drying has improved the stability and antioxidant activity of phenolic substances in ginger [14]. The combination of microwave and infrared drying has significantly improved the drying efficiency and uniformity of samples and effectively improved the quality and browning of ginger slices [15].

Ultrasound-assisted technology is a new, non-heating drying technology; it uses ultrasonic waves to conduct the liquid inside the sample and work on the liquid [16]. The liquid medium will produce cavitation in the compression stage, which will promote the migration of water in the cells, so as to shorten the drying time [17–19]. Compared with water bath ultrasound, airborne ultrasound has a higher uniformity in the energy transfer process, which effectively improves the drying quality and the texture structure of the sample, including kiwifruit [20], cumin seeds [21], mushroom [22], and orange peel [23]. In recent years, direct contact with ultrasound has played a significant role in improving the drying process due to its low energy attenuation; it can not only reduce the cell surface damage of dry samples and the mass transfer resistance during drying but also increase the retention rate of bioactive substances in the samples, thereby improving the antioxidant activity of the samples [24–27]. Drying using direct-contact ultrasound technology can retain more nutrients and bioactive substances, resulting in better performance of dried samples in both quality and function.

In this study, the direct-contact ultrasonic and far infrared combined drying technology was used to dry ginger. And, the effects of ultrasonic power, infrared drying temperature, and slice thickness on water migration, color, gingerol content, and antioxidant activity were investigated. Meanwhile, the volatile components were analyzed via gas ion mobility chromatography, in order to provide a technical basis for the industrialization of ginger drying.

2. Materials and Methods

2.1. Material and Chemicals

Fresh ginger was purchased from a local shop in Jinan (Shandong, China). Acetonitrile, methanol, and absolute ethyl alcohol were purchased from China Pharmaceutical Chemical Reagent Co., Ltd. (Shanghai, China); the reference substances of 6-gingerol and 8-gingerol were purchased from Shanghai Source Ye Technology Co., Ltd. (Shanghai, China). 2, 2-diphenyl-1-picrylhydrazyl (DPPH) was purchased from Sigma Aldrich (Shanghai, China).

2.2. Dehydrating Method

The direct-contact ultrasonic and far infrared combined drying system mainly includes a far infrared drying oven, ultrasonic generator (35 KHz), and ultrasonic oscillator (240 W) (i.e., three parts). The ultrasonic oscillator is placed in the center of the drying chamber of the infrared drying oven, and the energy transmission and conversion are carried out using the ultrasonic generator through the high temperature resistant connection line. The ultrasonic generator had a constant frequency of 35 KHz, and an adjustable power of 240 W, and the ultrasonic power was altered by adjusting the percentage of power. (Figure 1). The dry base moisture content of the ginger was (13.0627 g/g) when using the oven method at 105 °C. The fresh ginger was rinsed off and cut into thin slices of 4 mm by 6 mm. The ginger slices (80 slices, 4 mm by 6 mm) were laid flat on a disc in the direct-contact ultrasonic vibration disk (GSB-240, Ningbo Scientz Biotechnolody Co., Ltd., Ningbo, China) for the drying test. Briefly, the direct-contact ultrasonic disc was placed in an infrared drying oven (HF-881-2, Wujiang Huafei Electric Heating Equipment Co., Ltd., Suzhou, China) and different ultrasonic power states were set (Figure 1). The ginger slices were weighed every 10 min for the first 90 min and every 20 min for the period from 90 min to drying to constant weight. The temperature of the infrared was set into 30 °C, 40 °C, 50 °C, and 60 °C, respectively; additionally, the ultrasonic power was set to 0 W, 96 W, 144 W, 192 W,

and 240 W, respectively. Each experiment was repeated three times, and the average value was used for index analysis.

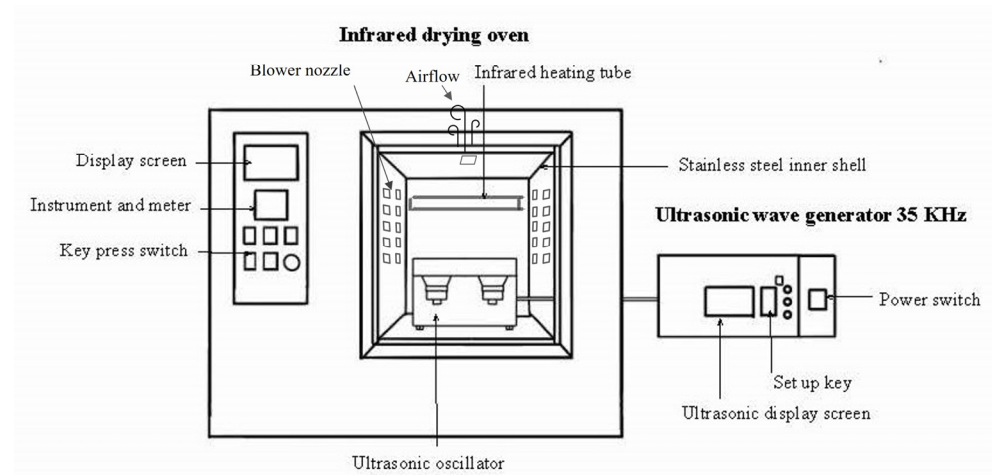


Figure 1. Direct-contact ultrasonic and far infrared combined drying equipment diagram.

2.3. Drying Characteristics

The drying characteristics of ginger with different drying methods were determined, including the drying base moisture content, moisture ratio, and drying rate [28].

2.3.1. Drying Base Moisture Content

The moisture content (M_C) of drying base in the direct-contact ultrasonic and far infrared combined drying process of ginger slices was calculated by using Equation (1) [29].

$$M_C = \frac{W_t - W_d}{W_d} \quad (1)$$

where M_C stands for the dry base moisture content (g/g) and W_t and W_d denote the drying sample weight (g) at random t time and the dried materials weight (g) after drying at 105 °C, respectively.

2.3.2. Moisture Ratio

The moisture ratio (M_R) of the drying base in the direct-contact ultrasonic and far infrared combined drying process of ginger slices was calculated by using Equation (2) [30].

$$M_R = \frac{M_t - M_e}{M_0 - M_e} \quad (2)$$

where the M_R represents the moisture ratio (g/g); M_t (g/g), M_0 (g/g,) and M_e (g/g) stand for the dry base moisture content of arbitrary time, the initial, and the constant weight, respectively.

2.3.3. Drying Rate

The drying rate (D_R) during the experiment of ginger slices was calculated by using Equation (3) [31].

$$D_R = \frac{M_t - M_{t+\Delta t}}{\Delta t} \quad (3)$$

where the D_R denotes the drying rate (g/g·h); the M_t and $M_{t+\Delta t}$ represent the moisture content (g/g) at the time of t and $t + \Delta t$, respectively.

2.4. LF-NMR Analysis

The transverse relaxation time of the samples was determined using LF-NMR analyzer (MesoMR23-60, Shanghai Niumai Electronic Technology Co., Ltd., Shanghai, China). Briefly, the samples were placed into the center of the radio-frequency coil with a diameter of 40 mm at the center of the permanent magnetic field. The multi-pulse echo sequence Carr–Purcell–Meiom–Gill (CPMG) was used to scan and collect the nuclear magnetic signals. Then, the Sirt algorithm was used for inversion with millions of iterations to obtain the T2 (the transverse relaxation time) spectrum. The main parameters of T2 included SF (main frequency)—20 MHz, O1 (offset frequency)—995,924.40 KHz, P1 (90-degree pulse time)—4.52 μ s, P2 (180-degree pulse time)—13.52 μ s, NS (cumulative sampling times)—8, TE (echo time)—1.000 ms, and NECH (echo number)—4000.

2.5. Chromatic Aberration

Chromatic aberration represents the surface color difference of samples treated using different methods which were measured using a NH310 high-quality portable colorimeter (Shenzhen 3 NH Technology Co. Ltd., Shenzhen, China). The CIE laboratory color parameters follow that the L^* is the brightness of the color, a^* is the degree of red and green, and b^* is the degree of yellow and blue. The change in the samples color was calculated by using Equation (4).

$$\Delta E = \sqrt{(L^*)^2 + (a^*)^2 + (b^*)^2} \quad (4)$$

where the ΔE stands for the total chromatic aberration. The ΔL^* , Δa^* , and Δb^* are the following calculation formulas:

$$\Delta L^* = L_t^* - L_0^*,$$

$$\Delta a^* = a_t^* - a_0^*,$$

$$\Delta b^* = b_t^* - b_0^*$$

where L_t^* , a_t^* , and b_t^* are the value of the color brightness, the red and green degree, and the yellow and blue degree for the materials at any time t when drying, respectively, while the L_0^* , a_0^* , and b_0^* denote the initial values that L^* , a^* , and b^* of the material, respectively.

2.6. Determination of Gingerol Content

Gingerol is a unique substance in ginger root, and the unique aromatic gingerol, such as 6-gingerol and 8-gingerol, has anti-inflammatory, anti-tumor, anti-oxidation, anti-coagulation, heart-strengthening, insecticidal, and other characteristic [32]. Firstly, the ginger extract was derived from dried samples for 6-gingerol and 8-gingerol content analysis. Briefly, crushed dried ginger (0.5 g) was mixed with ethanol solution (75%, 20 mL) and ultrasonic oscillation for 1 h (SB-5200DT, Ningbo Scientz Biotechnology Co., LTD), centrifugated ($1112 \times g$, 5 min, Thermo Fisher, Waltham, MA, USA) to obtain the supernatant, and then the extracted solution was freeze-dried for 48 h to obtain the alcohol extract solid (AEs). After that, the samples were stored in a refrigerator at 4 $^{\circ}$ C.

Specifically, 6-gingerol (0.0125 g) and 8-gingerol (0.0800 g) standards were dissolved in volumetric bottles (10 mL each) and constant diluted with anhydrous methanol of different concentration gradients as a standard solution to establish the 6-gingerol calibration curve ($y = 0.0002x + 0.0054$ $R^2 = 0.999$) and 8-gingerol calibration curve ($y = 0.0002x + 0.0044$ $R^2 = 0.999$), respectively [33]. The AEs were dissolved in the same manner. The absorbance was measured at 280 nm, and the blank was the anhydrous methanol solution.

The qualitative and quantitative analysis of gingerol in samples was carried out using 1120 HPLC (Agilent, Santa Clara, CA, USA) a 0.22 μ m syringe filter to filter the extract, and the filtrate was put into a liquid vial. Chromatographic condition: YMC-Pack ODS-AC18 column (250 \times 4.6 mm.D. S-5 μ m, 12 nm) at 45 $^{\circ}$ C; the gradient elution conditions were shown in Table 1. The flow rate was 1 mL/min, the sample volume was 5 μ L, and the detection wavelength was 280 nm. The measured value is put into the standard curve to obtain the gingerol content.

Table 1. The chromatographic elution conditions of standards and samples.

Time/min	Mobile Phase A: Water	Mobile Phase B: Acetonitrile
0	70	30
40	30	70

2.7. Analysis of Volatile Substances

The volatile substance of ginger was evaluated using a FlavourSpec[®] GC—IMS (Gas chromatography ion migration spectrometer, GAS, Dortmund, German). The sample (0.5 g) was added into the headspace solid phase bottle that kept 500 r/min incubation for 10 min at 80 °C. The headspace injection included an injection needle temperature (85 °C), injection volume (400 µL), SE-54 capillary-column chromatography (0.32 mm × 30 m, 0.25 µm), column temperature (60 °C), analysis time (35 min), high-purity nitrogen carrier gas (degree of purity ≥99.999%), carrier gas flow velocity (0.2 mL/min), drift gas velocity (50 mL/min), and IMS detector temperature (45 °C).

2.8. DPPH—Radical Scavenging Activity

The antioxidant activity of dried ginger was determined by measuring the DPPH (2, 2-diphenyl-1-picrylhydrazyl) radical scavenging ability [34]. The different dried gingers were ground to obtain a powder; the ginger powder (3.0 g) was mixed with ethanol (75%, 30 mL), ultrasonic extraction occurred for 30 min, and the mixture was centrifuged (3407 × g, 10 min). Then, the supernatant was collected and the procedure was repeated to extract the sediment twice [35]. Finally, the extracted solution was freeze-dried for 48 h and stored in a refrigerator at 4 °C. The DPPH radical scavenging activity was determined using microplate reader (Spark[®] MicroplateReader, TECAN, Männedorf, Switzerland). Briefly, the lyophilized samples (100 µL) were mixed with DPPH ethanol solution (0.15 mol/mL, 100 µL) and placed into a 96-well plate, the blank control was DPPH ethanol solution (100 µL) and sample solvent (100 µL). After incubation for 1 h in obscurity, the DPPH radical scavenging activity was assessed at the absorbance of 517 nm and calculated using Equation (5) [36].

$$DPPH \cdot (\%) = \frac{A_0 - A_1}{A_0} \quad (5)$$

where A_0 and A_1 represent the absorbance of blank and sample, respectively.

2.9. Statistical Analysis

The results are expressed as the mean ± standard deviation (SD) and were subjected to analysis of variance (ANOVA) tests in triplicate and the significant differences between diverse groups ($p < 0.05$). Origin 9.0 was used for data processing plotting. The laboratory analytical viewer (LAV) software was used in the analysis of sample chromatogram, and the difference chromatogram and fingerprint chromatogram of different samples were drawn by using the Reporter plug-in and Gallery Plot plug-in.

3. Results and Discussion

3.1. Effects of Drying Conditions on Drying Characteristics of Ginger

The effects of temperature, ultrasonic power, and thickness on the drying characteristics of ginger slices (4 mm) was determined by measuring the drying curve and drying rata curve. Drying to a constant weight was using as the basis for comparison, Figure 2a showed the changes of drying curves at different drying temperatures (30 °C, 40 °C, 50 °C, and 60 °C); the results showed that the drying time needed 400 min at the temperature of 30 °C, while the drying time at 50 °C and 60 °C only needed around 280 min. This indicated that the water loss rate of ginger slices was accelerated with the increase of temperature; consequently, the time to reach the inflection point was obviously shortened. The drying rate curve is shown in Figure 2b; the drying rate of the samples at the four experimental temperatures firstly increased and then decreased. And, the higher the temperature, the

faster the drying rate of the samples, indicating that increasing the drying temperature accelerates the water migration rate during drying [37]. Under the experimental temperature gradient, there is no significant difference in the variation in the appearance of ginger slices. From the perspective of the drying rate, there is trivial difference between the drying rate of 50 °C and 60 °C.

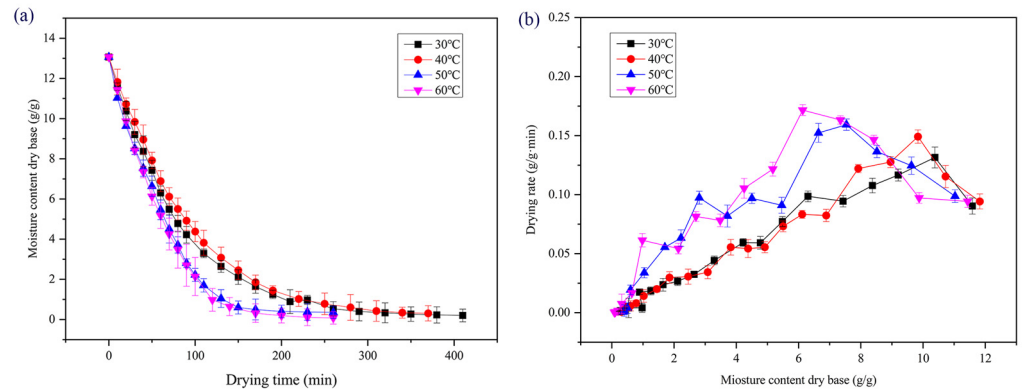


Figure 2. Drying curves and drying rate curves for different drying temperature. (a) Drying curves; (b) Drying rate curves.

The drying curves and drying rate curves of ginger slices (4 mm, 50 °C) at different ultrasonic powers (0 W, 96 W, 144 W, 192 W, and 240 W) changed with drying time, as shown in Figure 3. Based on drying to a constant weight, at the same drying temperature with the increase of ultrasonic power, the time for the moisture content of ginger slices to reach the drying inflection point was also significantly shortened. The drying time was 280 min at the ultrasonic power of 0 W but only around 160 min at 144 W, 192 W, and 240 W. The drying time was reduced by 42.8% after the addition of ultrasound, because the ultrasound could produce a cavitation effect in the internal tissues, which enlarged the internal water transport channels of ginger, accelerated the water loss rate and shortening the drying time [38]. The drying rate firstly increased and then decreased, because the ultrasonic gradually changed the internal texture of ginger slices at the initial stage [39], resulting in a slight increase in the drying rate (Figure 3b). In conclusion, ultrasonic power is also one of the main factors affecting the drying characteristics of ginger, and ultrasonic treatment can indeed have a significant effect on shortening the drying time. Under the ultrasonic power gradient of this experiment, the difference in the appearance of ginger slices is not obvious. From the drying rate, there was a slight difference between 144 W, 192 W, and 240 W.

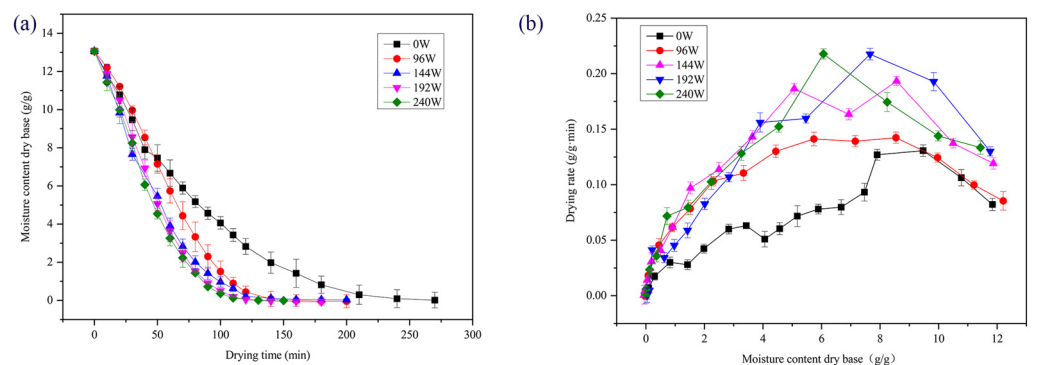


Figure 3. Drying curves and drying rate curves for different ultrasound frequencies. (a) Drying curves; (b) Drying rate curves.

The changes in the drying curve and drying rate curve against the drying time of ginger slices of different thicknesses (4 mm, 6 mm, 144 W, 50 °C) were shown in Figure 4. According to the analysis of the drying curve, under the premise that the drying temperature and ultrasonic power were the same and unchanged, the thinner the thickness of ginger slice, the faster the drying rate and the shorter the drying time. The ginger slices with a thickness of 4 mm were affected by ultrasonic conditions, while ginger slices with a thickness of 6 mm were less affected by ultrasonic factors. This was due to the fact that the thick slice led to the high resistance of water between cells in the diffusion process, which slows down the drying rate [40]. It can be concluded that, under the drying condition of 50 °C and 144 W, the thinner the ginger slice, the greater the degree of appearance change.

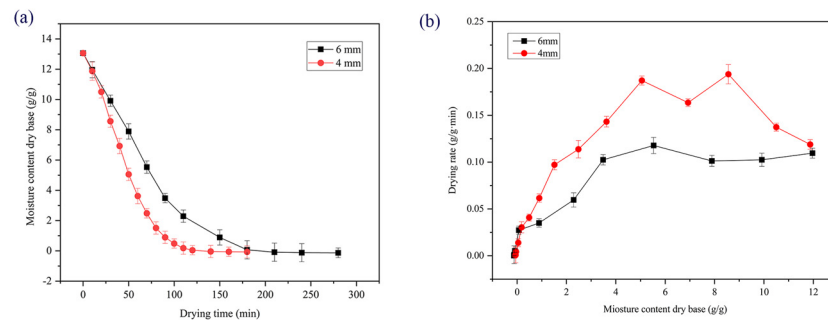


Figure 4. Drying curves and drying rate curves for different thickness. (a) Drying curves; (b) Drying rate curves.

3.2. Changes in Water Migration

LF-NMR (Low field nuclear magnetic resonance) technology was used to determine the changes in water migration of raw ginger slices [41]. In the drying process, the transverse relaxation time T_2 (transverse relaxation time) reflected the distribution and changes in the water content in different states [42], the smaller T (relaxation time) indicated the smaller degree of water freedom [43], indicating that water was more tightly bound to macromolecules in the environment in which it was located and less easily removed. The greater the T_2 , the greater the water freedom and the easier the removal [44]. The magnetic resonance signal data of ginger slices under different drying methods were fitted using multi-exponential fitting to obtain the T_2 inversion map. The LF-MRI signal data of ginger slices (6 mm) dried at 50 °C, 0 W and 50 °C, 144 W were fitted via multi-exponential fitting to obtain T_2 inversion plots, as shown in Figure 5. The water sources in raw ginger slices were free water and non-flowing water and had a low content of bound water. During the drying process, it was observed that the position of the peak of water in different states obviously shifted to the left, indicating that the mobility of water in the ginger slices became worse. The free water was lost rapidly during the drying process, while the non-flowing water was lost slowly. The bound water almost did not change before and during the middle period of drying and began to lose the bound water when the free water and non-flowing water were lost [45].

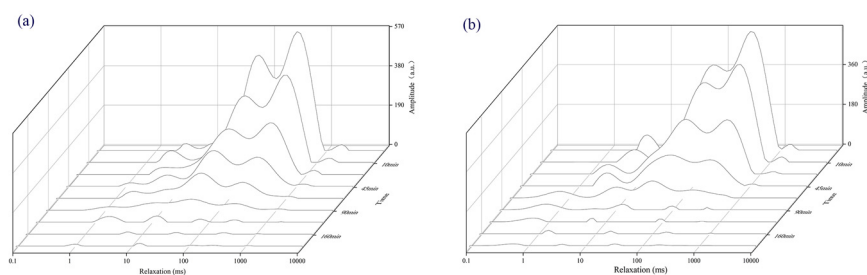


Figure 5. The T_2 inversion plots at different ultrasound frequencies. (a) 6 mm, 50 °C, 0 W; (b) 6 mm, 50 °C, 144 W.

From T_2 inversion plots, the content and loss rate of non-flowing water (especially after 45 min) of ginger slices dried using direct-contact ultrasonic and far infrared combined drying were faster than those of ginger slices dried using traditional infrared drying. This is because the ultrasonic energy increased the freedom of immobile water, making it easier to lose and, thus, increasing the drying rate [46]. Moreover, from the above comparison, it can be concluded that the drying time of direct-contact ultrasound and far infrared combined drying ginger slices is shorter than that of traditional infrared drying. A large part of the reason is that the immobile water in direct-contact ultrasound and far infrared combined drying ginger slices is converted into the kinetic energy of water due to the energy generated via ultrasound [47], thus accelerating the migration rate of water and shortening the drying time.

3.3. Effects of Different Drying Conditions on Color Changes of Ginger Slices

Color is an important index affecting sample quality; the influence of different drying temperatures on the color of the sample was shown in Figure 6a, where L^* represented the brightness difference, a^* represented the red–green degree, b^* represented the blue–violet degree, and ΔE was used to evaluate the overall color change. Compared with the fresh sample, the L^* value on the surface of the dried ginger increased, indicating that the brightness of dried ginger was higher than that of fresh ginger, which was due to reduce the water content of the sample after drying, leading to increased brightness [48]. In general, the surface L^* value was the lowest, the a^* value was the largest, and the ΔE value was the smallest at the drying temperature of 30 °C. This is due to the longer drying time required under drying conditions at 30 °C and the longer contact time of ginger with air. However, the drying temperature of 60 °C is higher, which causes the cell rupture of ginger to release oxidase, resulting in a high degree of browning of ginger slices [49]. The L^* value of 40 °C and 50 °C drying conditions is higher, and the color of dried ginger slices is better, while the b^* value of 40 °C drying ginger slices is larger, so the drying effect is the best under the drying temperature of 50 °C.

Figure 6b showed the influence of different ultrasonic powers on color change when the drying temperature was constant. At 0 W and 240 W ultrasonic powers, the L^* value was the lowest, a^* value was the largest, and ΔE value was the smallest on the surface of the dry sample. The former is due to the absence of ultrasonic treatment, which puts the ginger in contact with the air for a long time, resulting in a high degree of ginger browning, while the ultrasonic energy at 240 W power is overtop, which causes the ginger cells to break down and release oxidase, resulting in a high degree of ginger browning [50]. Under the condition of 144 W ultrasonic drying, the L^* value was the highest, the a^* was small, the ΔE value was the largest, and the color of dried ginger slices was better.

Figure 6c showed the influence of slice thickness on color change when the drying temperature and ultrasonic frequency were constant. The L^* value of the dry sample with 6 mm slices was larger than that with 4 mm slices, while the a^* value was smaller and the ΔE value was larger. The thin section of the 4 mm sample makes it easier for the ultrasonic energy to penetrate the cells and rupture them, releasing the oxidase and resulting in a high degree of browning [51]. However, the dried samples of 6 mm slices had less cell rupture and less browning than those of 4 mm slices due to the thicker thickness. Therefore, the color of ginger slices under the drying conditions of 6 mm size, 144 W ultrasonic power, and 50 °C drying temperature is the best.

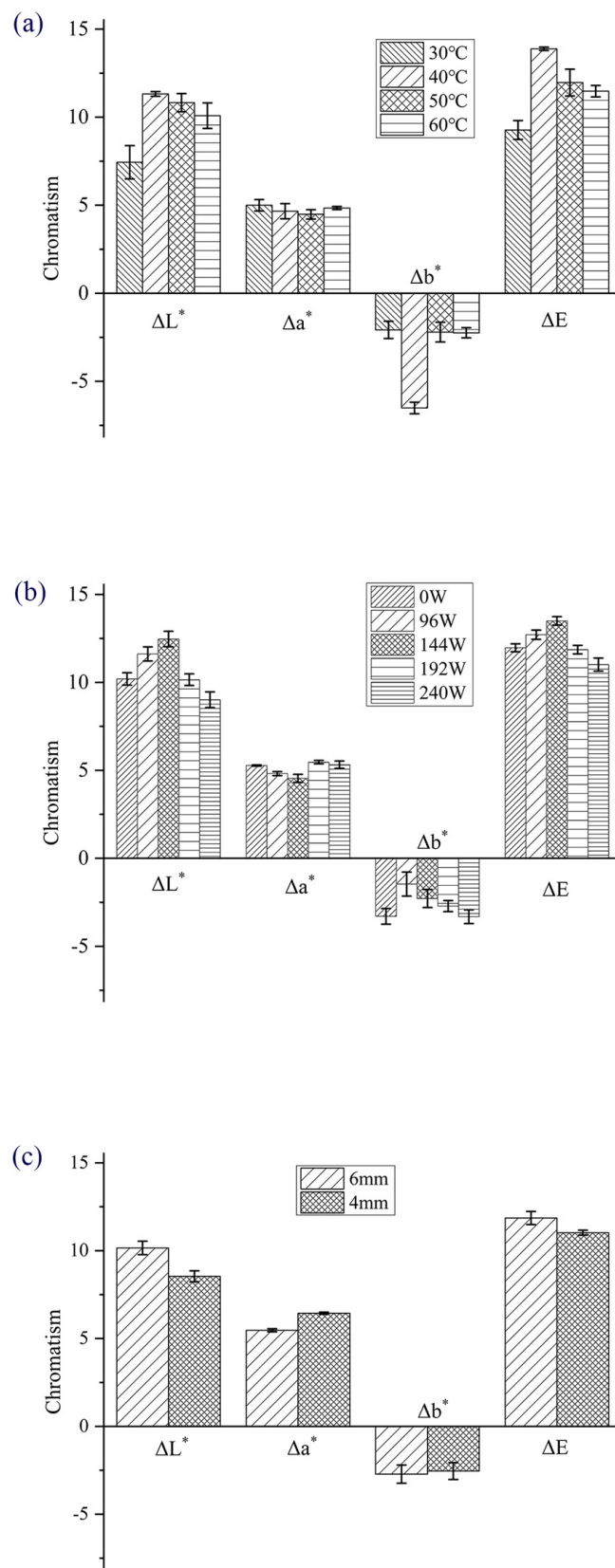


Figure 6. The chromatism of different drying conditions: (a) Different drying temperature; (b) Different ultrasonic frequencies; (c) Different thickness.

3.4. Effects of Different Drying Methods on Gingerol Content

According to the set chromatographic conditions, 10 μL each of the control solution (standard solution) and the sample solution (6 mm, 50 $^{\circ}\text{C}$, and 0 W; 6 mm, 50 $^{\circ}\text{C}$, and 144 W; 4 mm, 50 $^{\circ}\text{C}$, and 0 W; and 4 mm, 50 $^{\circ}\text{C}$, and 144 W) were precisely extracted, and the sample was injected using an automatic sampler. The chromatographic diagrams of the standard and sample solution are shown in Figure 7. The content of 6-gingerol and 8-gingerol in ginger slices under different drying conditions was shown in Table 2. At the drying temperature of 50 $^{\circ}\text{C}$, under the thinner slice thickness (4 mm), the gingerol content of the ultrasonic treated ginger slices ($0.0160 \pm 0.0006 \text{ mg/g}$) is lower than that of the infrared dried ginger slices ($0.0214 \pm 0.0018 \text{ mg/g}$), which may be due to the mechanical damage inside the material due to cavitation and mechanical effects caused by high-intensity ultrasound, reducing the content of active ingredients [52]. However, with the increase of slice thickness (6 mm), the gingerol content ($0.0205 \pm 0.0008 \text{ mg/g}$) was higher than that of ginger slices dried using infrared drying methods ($0.0194 \pm 0.0015 \text{ mg/g}$), which may be due to the ability of ginger slices with a certain thickness to reduce the damage of the internal cellular structure of the material caused by ultrasound [53]. The 6 mm, 144 W ginger showed satisfactory results in terms of drying time, retention of volatile oil, and sample color.

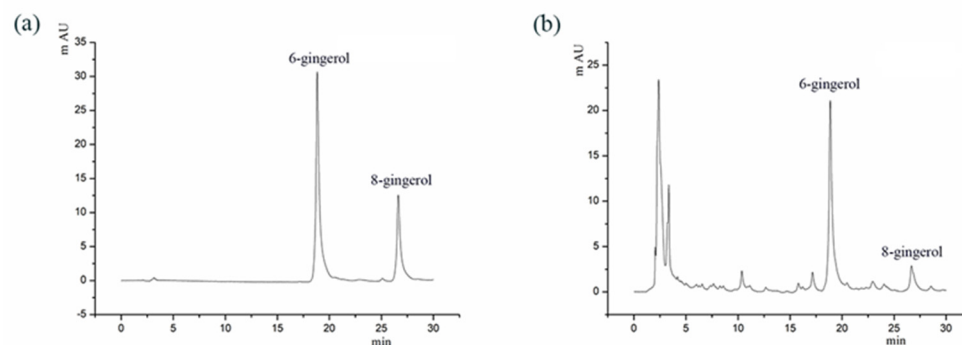


Figure 7. The chromatogram of 6-gingerol and 8-gingerol: (a) 6-gingerol and 8-gingerol standards; (b) 6 mm, 50 $^{\circ}\text{C}$, and 144 W conditions.

Table 2. The gingerol content, drying time, and chromatism of ginger slices under different slice thickness and ultrasonic frequency (at 50 $^{\circ}\text{C}$).

	4 mm		6 mm	
	0 W	144 W	0 W	144 W
6-gingerol (mg/g)	0.1012 ± 0.0171^a	0.1017 ± 0.0831^a	0.0910 ± 0.0147^b	0.1063 ± 0.0104^a
8-gingerol (mg/g)	0.0214 ± 0.0018^a	0.0160 ± 0.0006^b	0.0194 ± 0.0015^a	0.0205 ± 0.0008^a
Drying time (min)	280 ^b	160 ^d	430 ^a	270 ^c
Chromatism (ΔE)	11.97 ± 0.65^a	11.86 ± 0.58^b	11.62 ± 0.79^c	11.03 ± 0.91^d

Each value is the mean \pm standard deviation ($n = 3$). Different letters (^{a-d}) are significantly different ($p < 0.05$).

3.5. Analysis of Volatile Substances

The GC-IMS (gas chromatography-ion migration spectrometer) analysis was used to detect and analyze volatile substances in ginger slices dried using two different methods. The difference in volatile components (VOCs) in ginger dried using different methods was qualitatively analyzed using the Reporter plug-in in LAV software, as shown in Figure 8a, where the abscissa represents the ion migration time and the ordinate represents the retention time; each red dot represents a volatile substance, with darker colors indicating higher levels [54]. The results showed that the content of VOCs in the samples treated with ultrasonic combined with infrared drying was higher than that of the samples treated with infrared drying. This may be due to the fact that ultrasonic treatment shortened

Table 3. There are many volatile compounds in ginger, including aldehydes, ketones, alcohols, esters, and pyrazines.

NO	Compounds	CAS#	Formula	MW	RI	Rt	Dt
1	Nonanal	124-19-6	C ₉ H ₁₈ O	142.2	1103.2	798.551	14.786
2	1,8-Cineole	470-82-6	C ₁₀ H ₁₈ O	154.3	1037.7	674.219	12.958
3	Limonene	138-86-3	C ₁₀ H ₁₆	136.2	1034.2	668.154	12.194
4	Octanal	124-13-0	C ₈ H ₁₆ O	128.2	1009.5	626.709	14.102
5	Butyl butyrate	109-21-7	C ₈ H ₁₆ O ₂	144.2	996.8	606.492	1.221
6	Δ-3-Carene	13466-78-9	C ₁₀ H ₁₆	136.2	1011.9	630.753	12.178
7	Myrcene	123-35-3	C ₁₀ H ₁₆	136.2	991.8	595.373	11.733
8	β-Pinene	127-91-3	C ₁₀ H ₁₆	136.2	979.0	567.07	12.178
9	α-Fenchene	471-84-1	C ₁₀ H ₁₆	136.2	952.4	512.485	12.147
10	α-Pinene	80-56-8	C ₁₀ H ₁₆	136.2	937.0	483.17	12.194
11	2-Heptanone	110-43-0	C ₇ H ₁₄ O	114.2	890.3	404.325	16.297
12	Heptanal	111-71-7	C ₇ H ₁₄ O	114.2	901.7	422.52	13.387
13	Cyclohexanone	108-94-1	C ₆ H ₁₀ O	98.1	889.8	403.43	11.573
14	1-Hexanol	111-27-3	C ₆ H ₁₄ O	102.2	868.9	369.358	1.124
15	(Z)-3-hexen-1-ol	928-96-1	C ₆ H ₁₂ O	100.2	852.2	344.223	11.798
16	Hexanal	66-25-1	C ₆ H ₁₂ O	100.2	793.6	268.818	1.565
17	Butyl methyl ketone	591-78-6	C ₆ H ₁₂ O	100.2	781.5	255.412	11.887
18	1-Butanol, 2-methyl-	137-32-6	C ₅ H ₁₂ O	88.1	740.1	214.638	11.536
19	1-Hexen-3-one	1629-60-3	C ₆ H ₁₀ O	98.1	776.2	249.827	10.904
20	1-Pentanol	71410	C ₅ H ₁₂ O	88.1	758.0	231.395	1.255
21	Pentanal	110-62-3	C ₅ H ₁₀ O	86.1	691.4	174.98	14.225
22	1-Butanol	71-36-3	C ₄ H ₁₀ O	74.1	651.2	156.548	13.965
23	Pentan-2,3-dione	600-14-6	C ₅ H ₈ O ₂	100.1	692.2	175.539	12.931
24	2,3 Butandione (Diacetyl)	431-03-8	C ₄ H ₆ O ₂	86.1	572.4	126.945	11.556
25	Linalool	78-70-6	C ₁₀ H ₁₈ O	154.3	1087.9	767.519	12.229
26	1-Octen-3-ol	3391-86-4	C ₈ H ₁₆ O	128.2	991.4	594.422	11.786
27	Benzaldehyde	100-52-7	C ₇ H ₆ O	106.1	960.1	527.625	11.508
28	Styrene	100-42-5	C ₈ H ₈	104.2	902.2	423.356	1.441
29	3-Hexen-1-ol	928-96-1	C ₆ H ₁₂ O	100.2	841.4	328.862	1.223
30	2-Pentanone	107-87-9	C ₅ H ₁₀ O	86.1	676.5	167.452	11.097
31	Isopropyl acetate	108-21-4	C ₅ H ₁₀ O ₂	102.1	660.5	160.477	11.593
32	Acetone	67-64-1	C ₃ H ₆ O	58.1	506.1	106.417	11.142
33	Propanal	123-38-6	C ₃ H ₆ O	58.1	489.6	101.839	10.425
34	n-Nonanal	124-19-6	C ₉ H ₁₈ O	142.2	1103.5	799.136	19.427
35	2-Nonanone	821-55-6	C ₉ H ₁₈ O	142.2	1092.6	776.93	14.109
36	Octamethylcyclotetrasiloxane	556-67-2	C ₈ H ₂₄ O ₄ Si ₄	296.6	1011.8	630.574	16.845
37	2,3-Butanedione	431-03-8	C ₄ H ₆ O ₂	86.1	567.9	125.429	11.661
38	1-Propanol	71-23-8	C ₃ H ₈ O	60.1	561.6	123.365	11.248
39	Ethyl Acetate	141-78-6	C ₄ H ₈ O ₂	88.1	596.2	135.234	10.953
40	Terpinolene	586-62-9	C ₁₀ H ₁₆	136.2	1090.1	768.204	1.22084
41	Benzeneacetaldehyde	122-78-1	C ₈ H ₈ O	120.2	1045.9	687.765	1.2561
42	β-Ocimene	13877-91-3	C ₁₀ H ₁₆	136.2	1035.1	669.436	1.21916
43	Hexyl acetate	142-92-7	C ₈ H ₁₆ O ₂	144.2	1010.1	628.708	1.40889
44	Pyrazine, 2-ethyl-5-methyl-	13360-64-0	C ₇ H ₁₀ N ₂	122.2	991.9	597.143	1.1755
45	Camphene	79-92-5	C ₁₀ H ₁₆	136.2	951.9	511.612	1.21412
46	2-Propanol	67-63-0	C ₃ H ₈ O	60.1	929.3	468.846	1.20572
47	3-Methylbutanal	590-86-3	C ₅ H ₁₀ O	86.1	902.6	423.026	1.20069
48	Dipropyl sulfide	111-47-7	C ₆ H ₁₄ S	118.2	889.4	401.644	1.15703
49	Butanal	123-72-8	C ₄ H ₈ O	72.1	868.3	367.024	1.12513
50	2-Hexenal	505-57-7	C ₆ H ₁₀ O	98.1	852.1	342.586	1.18054
51	(Z)-3-Hexen-1-ol	928-96-1	C ₆ H ₁₂ O	100.2	839.9	325.277	1.22419
52	Furfural	1998/1/1	C ₅ H ₄ O ₂	96.1	834	317.131	1.33333
53	1-Octene	111-66-0	C ₈ H ₁₆	112.2	784.7	257.056	1.19061
54	2,3-Pentanedione	600-14-6	C ₅ H ₈ O ₂	100.1	673.1	163.379	1.27792
55	2-Propenal, 2-methyl-	78-85-3	C ₄ H ₆ O	70.1	582.5	127.741	1.22251

3.6. DPPH—Radical Scavenging Activity

The minimum concentration of ginger slices under different ultrasonic power and slice thickness (at 50 °C) to reach IC_{50} can explain the antioxidant capacity of the sample to a certain extent. The antioxidant activities of four different specifications of ginger slices were exhibited in Figure 9. The antioxidant capacity of the four samples with different specifications was shown as 6 mm, 144 W > 4 mm, 144 W > 4 mm, 0 W > 6 mm, 0 W ($p < 0.05$). The IC_{50} (half-inhibition concentration) values of 6 mm, 144 W; 4 mm, 144 W; 4 mm, 0 W; and 6 mm, 0 W were 0.402 ± 0.006 mg/mL, 0.456 ± 0.011 mg/mL, 0.724 ± 0.009 mg/mL, and 0.843 ± 0.008 mg/mL ($p < 0.05$), respectively. From the experimental data, the DPPH scavenging capacity of the samples treated via sonication was significantly enhanced. According to Sections 3.4 and 3.5 gingerol content data and volatile substance content comparison, it was found that the content of ultrasonic-treated samples was higher than that of non-ultrasonic samples, and the content of 6mm samples after ultrasonic treatment was higher than that of 4mm samples. This may be due to the fact that ultrasonic combined with infrared drying shortened the drying time and improved the retention of active substances.

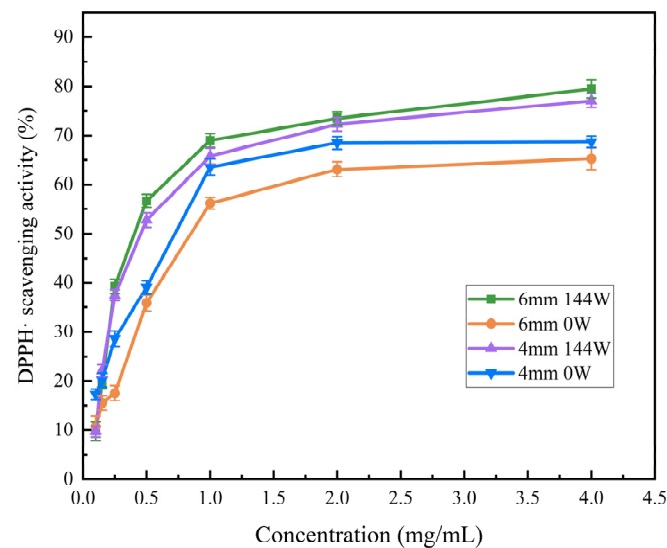


Figure 9. The antioxidant activity at different ultrasound frequencies and specifications of ginger at 50 °C.

4. Conclusions

In this study, the drying rate, water transport, gingerol content, flavor, and antioxidant activity of ginger slices under different drying conditions were investigated using direct-contact ultrasound and far infrared combined drying. The results of LF-NMR showed that ultrasonic treatment increased the degree of freedom of hard-to-flow water and accelerated the drying rate, which provided auxiliary proof for the direct-contact ultrasound and far infrared combined drying technology of ginger slices. The GC-IMS data indicate that direct exposure to combined ultrasonic and far infrared drying increases the retention of volatile components in the sample. The gingerol content of the thicker slices treated with ultrasound was higher than that of the non-sonicated slices. Compared with the traditional infrared drying, ultrasonic and far infrared combined drying improved the drying rate of ginger slices, shortened the drying time, reduced the color difference, and improved the antioxidant activity of ginger slices. Therefore, the direct-contact ultrasonic and far infrared combined drying technology has a certain reference significance for the drying process of ginger slices.

Author Contributions: Conceptualization, Z.F. and F.L.; methodology, Z.F., M.Z. and F.L.; software, Z.F., M.Z., R.S. and F.L.; validation, L.G., X.W. and F.L.; formal analysis, Z.F.; investigation, Z.F. and F.L.; resources, L.G., X.W. and F.L.; data curation, Z.F. and F.L.; writing—original draft preparation, Z.F.; writing—review and editing, M.Z., L.G., R.S., X.W. and F.L.; visualization, Z.F., M.Z., R.S. and F.L.; supervision, L.G., X.W., and F.L.; project administration, Z.F., M.Z., L.G., R.S., X.W. and F.L.; funding acquisition, F.L. All authors have read and agreed to the published version of the manuscript.

Funding: This research was funded by the scientific and technological innovation project of China Academy of Chinese Medical Sciences (CI2021B013); new innovative team of Jinan (202228020); Education and Industry Integration Innovation Pilot Project from Qilu University of Technology (Shandong Academy of Sciences) (2022JBZ02-04); China Agriculture Research System of MOF and MARA (CARS-21); and Shandong Province Taishan Scholar Program (X.W.).

Data Availability Statement: All data generated or analyzed during this study are included in this published article.

Conflicts of Interest: Author Rencai Shao was employed by the company Ningbo Scientz Biotechnology Co., Ltd. The remaining authors declare that the research was conducted in the absence of any commercial or financial relationships that could be construed as a potential conflict of interest.

References

- Malik, A.; Shimpy; Kumar, M. Advancements in ginger drying technologies. *J. Stored Prod. Res.* **2023**, *100*, 102058. [[CrossRef](#)]
- Pei, Y.; Li, Z.; Song, C.; Li, J.; Xu, W.; Zhu, G. Analysis and modelling of temperature and moisture gradient for ginger slices in hot air drying. *J. Food Eng.* **2022**, *323*, 111009. [[CrossRef](#)]
- Chen, D.; Pan, S.; Chen, J.; Pang, X.; Guo, X.; Gao, L.; Liao, X.; Wu, J. Comparing the Effects of High Hydrostatic Pressure and Ultrahigh Temperature on Quality and Shelf Life of Cloudy Ginger Juice. *Food Bioprocess Technol.* **2016**, *9*, 1779–1793. [[CrossRef](#)]
- Kiyama, R. Nutritional implications of ginger: Chemistry, biological activities and signaling pathways. *J. Nutr. Biochem.* **2020**, *86*, 108486. [[CrossRef](#)] [[PubMed](#)]
- Amponsah, I.K.; Boakyee, A.; Orman, E.; Armah, F.A.; Borquaye, L.S.; Adjei, S.; Dwamena, Y.A.; Baah, K.A.; Harley, B.K. Assessment of some quality parameters and chemometric-assisted FTIR spectral analysis of commercial powdered ginger products on the Ghanaian market. *Heliyon* **2022**, *8*, e09150. [[CrossRef](#)] [[PubMed](#)]
- Zeng, S.; Wang, B.; Lv, W.; Wu, Y. Effects of microwave power and hot air temperature on the physicochemical properties of dried ginger (*Zingiber officinale*) using microwave hot-air rolling drying. *Food Chem.* **2023**, *404*, 134741. [[CrossRef](#)]
- Suhag, R.; Singh, S.; Kumar, Y.; Prabhakar, P.K.; Meghwal, M. Microfluidization of Ginger Rhizome (*Zingiber officinale* Roscoe) Juice: Impact of Pressure and Cycles on Physicochemical Attributes, Antioxidant, Microbial, and Enzymatic Activity. *Food Bioprocess Technol.* **2023**. [[CrossRef](#)]
- Liu, Z.-L.; Staniszevska, I.; Zielinska, D.; Zhou, Y.-H.; Nowak, K.W.; Xiao, H.-W.; Pan, Z.; Zielinska, M. Combined Hot Air and Microwave-Vacuum Drying of Cranberries: Effects of Pretreatments and Pulsed Vacuum Osmotic Dehydration on Drying Kinetics and Physicochemical Properties. *Food Bioprocess Technol.* **2020**, *13*, 1848–1856. [[CrossRef](#)]
- Yan, W.; Liu, Q.; Wang, Y.; Tao, T.; Liu, B.; Liu, J.; Ding, C. Inhibition of Lipid and Aroma Deterioration in Rice Bran by Infrared Heating. *Food Bioprocess Technol.* **2020**, *13*, 1677–1687. [[CrossRef](#)]
- Bai, R.; Sun, J.; Qiao, X.; Zheng, Z.; Li, M.; Zhang, B. Hot Air Convective Drying of Ginger Slices: Drying Behaviour, Quality Characteristics, Optimisation of Parameters, and Volatile Fingerprints Analysis. *Foods* **2023**, *12*, 1283. [[CrossRef](#)]
- Shofinita, D.; Lestari, D.; Aliwarga, L.; Sumampouw, G.A.; Ambarwati, S.A.; Gunawan, K.C.; Achmadi, A.B. Drying Methods of Coffee Extracts and Their Effects on Physicochemical Properties: A Review. *Food Bioprocess Technol.* **2023**. [[CrossRef](#)]
- Zhang, D.; Huang, D.; Zhang, Y.; Lu, Y.; Huang, S.; Gong, G.; Li, L. Ultrasonic assisted far infrared drying characteristics and energy consumption of ginger slices. *Ultrason. Sonochem.* **2023**, *92*, 106287. [[CrossRef](#)] [[PubMed](#)]
- E, J.; R, V.; T, J.Z. Quality of dry ginger (*Zingiber officinale*) by different drying methods. *J. Food Sci. Technol.* **2012**, *51*, 3190–3198. [[CrossRef](#)] [[PubMed](#)]
- An, K.; Wei, L.; Fu, M.; Cheng, L.; Peng, J.; Wu, J. Effect of Carbonic Maceration (CM) on the Vacuum Microwave Drying of Chinese Ginger (*Zingiber officinale* Roscoe) Slices: Drying Characteristic, Moisture Migration, Antioxidant Activity, and Microstructure. *Food Bioprocess Technol.* **2020**, *13*, 1661–1674. [[CrossRef](#)]
- Zeng, S.; Wang, B.; Zhao, D.; Lv, W. Microwave infrared vibrating bed drying of ginger: Drying qualities, microstructure and browning mechanism. *Food Chem.* **2023**, *424*, 136340. [[CrossRef](#)] [[PubMed](#)]
- Kahraman, O.; Malvandi, A.; Vargas, L.; Feng, H. Drying characteristics and quality attributes of apple slices dried by a non-thermal ultrasonic contact drying method. *Ultrason. Sonochem.* **2021**, *73*, 105510. [[CrossRef](#)] [[PubMed](#)]
- Akhoundzadeh Yamchi, A.; Yeganeh, R.; Kouchakzadeh, A. Effect of ultrasonic pretreatment on drying kinetics and physio-mechanical characteristics of peach slices. *J. Food Process Eng.* **2022**, *45*, e14053. [[CrossRef](#)]
- Rani, P.; Tripathy, P.P. Effect of ultrasound and chemical pretreatment on drying characteristics and quality attributes of hot air dried pineapple slices. *J. Food Sci. Technol.* **2019**, *56*, 4911–4924. [[CrossRef](#)]

19. Rodríguez, Ó.; Llabrés, P.J.; Simal, S.; Femenia, A.; Rosselló, C. Intensification of Predrying Treatments by Means of Ultrasonic Assistance: Effects on Water Mobility, PPO Activity, Microstructure, and Drying Kinetics of Apple. *Food Bioprocess Technol.* **2014**, *8*, 503–515. [[CrossRef](#)]
20. Llavata, B.; Femenia, A.; Clemente, G.; Cárcel, J.A. Combined Effect of Airborne Ultrasound and Temperature on the Drying Kinetics and Quality Properties of Kiwifruit (*Actinidia deliciosa*). *Food Bioprocess Technol.* **2023**. [[CrossRef](#)]
21. Namjoo, M.; Moradi, M.; Dibagar, N.; Niakousari, M. Cold Plasma Pretreatment Prior to Ultrasound-assisted Air Drying of Cumin Seeds. *Food Bioprocess Technol.* **2022**, *15*, 2065–2083. [[CrossRef](#)]
22. Vallespir, F.; Crescenzo, L.; Rodríguez, Ó.; Marra, F.; Simal, S. Intensification of Low-Temperature Drying of Mushroom by Means of Power Ultrasound: Effects on Drying Kinetics and Quality Parameters. *Food Bioprocess Technol.* **2019**, *12*, 839–851. [[CrossRef](#)]
23. Garcia-Perez, J.V.; Ortuño, C.; Puig, A.; Carcel, J.A.; Perez-Munuera, I. Enhancement of Water Transport and Microstructural Changes Induced by High-Intensity Ultrasound Application on Orange Peel Drying. *Food Bioprocess Technol.* **2011**, *5*, 2256–2265. [[CrossRef](#)]
24. Zang, Z.; Zhang, Q.; Huang, X.; Jiang, C.; He, C.; Wan, F. Effect of Ultrasonic Combined with Vacuum Far-infrared on the Drying Characteristics and Physicochemical Quality of Angelica sinensis. *Food Bioprocess Technol.* **2023**, *16*, 2455–2470. [[CrossRef](#)]
25. Xu, J.; Wang, D.; Lei, Y.; Cheng, L.; Zhuang, W.; Tian, Y. Effects of combined ultrasonic and microwave vacuum drying on drying characteristics and physicochemical properties of Tremella fuciformis. *Ultrason. Sonochem.* **2022**, *84*, 105963. [[CrossRef](#)] [[PubMed](#)]
26. Zhang, Q.; Wan, F.; Zang, Z.; Jiang, C.; Xu, Y.; Huang, X. Effect of ultrasonic far-infrared synergistic drying on the characteristics and qualities of wolfberry (*Lycium barbarum* L.). *Ultrason. Sonochem.* **2022**, *89*, 106134. [[CrossRef](#)]
27. Liu, Y.; Zeng, Y.; Hu, X.; Sun, X. Effect of Ultrasonic Power on Water Removal Kinetics and Moisture Migration of Kiwifruit Slices During Contact Ultrasound Intensified Heat Pump Drying. *Food Bioprocess Technol.* **2020**, *13*, 430–441. [[CrossRef](#)]
28. Gu, C.; Ma, H.; Tuly, J.A.; Guo, L.; Zhang, X.; Liu, D.; Ouyang, N.; Luo, X.; Shan, Y. Effects of catalytic infrared drying in combination with hot air drying and freeze drying on the drying characteristics and product quality of chives. *Lwt* **2022**, *161*, 113363. [[CrossRef](#)]
29. Dajbych, O.; Kabutey, A.; Mizera, Č.; Herák, D. Investigation of the Effects of Infrared and Hot Air Oven Drying Methods on Drying Behaviour and Colour Parameters of Red Delicious Apple Slices. *Processes* **2023**, *11*, 3027. [[CrossRef](#)]
30. Reis, C.G.d.; Figueirêdo, R.M.F.d.; Queiroz, A.J.d.M.; Paiva, Y.F.; Amadeu, L.T.S.; Santos, F.S.d.; Ferreira, J.P.d.L.; Lima, T.L.B.d.; Andrade, F.S.; Gomes, J.P.; et al. Pineapple Peel Flours: Drying Kinetics, Thermodynamic Properties, and Physicochemical Characterization. *Processes* **2023**, *11*, 3161. [[CrossRef](#)]
31. Macedo, L.L.; Vimercati, W.C.; da Silva Araújo, C.; Saraiva, S.H.; Teixeira, L.J.Q. Effect of drying air temperature on drying kinetics and physicochemical characteristics of dried banana. *J. Food Process Eng.* **2020**, *43*, e13451. [[CrossRef](#)]
32. Feng, Y.; Ping Tan, C.; Zhou, C.; Yagoub, A.E.A.; Xu, B.; Sun, Y.; Ma, H.; Xu, X.; Yu, X. Effect of freeze-thaw cycles pretreatment on the vacuum freeze-drying process and physicochemical properties of the dried garlic slices. *Food Chem.* **2020**, *324*, 126883. [[CrossRef](#)] [[PubMed](#)]
33. He, L.; Duan, H.; Chen, X.; Chen, Y.; Mo, Q.; Huang, J.; Zhao, H.; Yao, X.; Chen, J.; Yao, Z. Quality assessment of commercial dried ginger (*Zingiber officinale Roscoe*) based on targeted and non-targeted chemical profiles and anti-inflammatory activity. *Food Res. Int.* **2023**, *166*, 112589. [[CrossRef](#)] [[PubMed](#)]
34. Wang, C.-Y.; Chen, Y.-W.; Hou, C.-Y. Antioxidant and antibacterial activity of seven predominant terpenoids. *Int. J. Food Prop.* **2019**, *22*, 230–238. [[CrossRef](#)]
35. Mustafa, I.; Chin, N.L. Antioxidant Properties of Dried Ginger (*Zingiber officinale Roscoe*) var. Bentong. *Foods* **2023**, *12*, 178. [[CrossRef](#)] [[PubMed](#)]
36. Akther, F.; Alim, M.A.; Nasrin, N.A.; Khan, M.; Gomes, D.N.; Suhan, M.; Islam, M.; Begum, R. Effects of different drying methods on the proximate composition, antioxidant activity, and phytochemical content of *Hibiscus sabdariffa* L. Calyx. *Food Chem. Adv.* **2023**, *3*, 100553. [[CrossRef](#)]
37. Mahayothee, B.; Thamsala, T.; Khuwijitjaru, P.; Janjai, S. Effect of drying temperature and drying method on drying rate and bioactive compounds in cassumunar ginger (*Zingiber montanum*). *J. Appl. Res. Med. Aromat. Plants* **2020**, *18*, 100262. [[CrossRef](#)]
38. Kaur, M.; Modi, V.K.; Sharma, H.K. Evaluation of ultrasonication and carbonation-ultrasonication assisted convective drying techniques for enhancing the drying rates and quality parameters of ripe and raw banana (*Musa*) peel. *J. Food Sci. Technol.* **2022**, *59*, 4542–4552. [[CrossRef](#)]
39. Xi, H.; Liu, Y.; Guo, L.; Hu, R. Effect of ultrasonic power on drying process and quality properties of far-infrared radiation drying on potato slices. *Food Sci. Biotechnol.* **2019**, *29*, 93–101. [[CrossRef](#)]
40. Li, C.; Ren, G.; Zhang, L.; Duan, X.; Wang, Z.; Ren, X.; Chu, Q.; He, T. Effects of different drying methods on the drying characteristics and drying quality of *Cistanche deserticola*. *Lwt* **2023**, *184*, 115000. [[CrossRef](#)]
41. Sun, Q.; Zhang, M.; Mujumdar, A.S.; Yu, D. Research on the Vegetable Shrinkage During Drying and Characterization and Control Based on LF-NMR. *Food Bioprocess Technol.* **2022**, *15*, 2776–2788. [[CrossRef](#)]
42. Wang, H.; Che, G.; Wan, L.; Wang, X.; Tang, H. Combination of LF-NMR and BP-ANN to monitor the moisture content of rice during hot-air drying. *J. Food Process Eng.* **2022**, *45*, e14102. [[CrossRef](#)]
43. Liu, W.; Zhang, M.; Bhandari, B.; Yu, D. A novel combination of LF-NMR and NIR to intelligent control in pulse-spouted microwave freeze drying of blueberry. *Lwt* **2021**, *137*, 110455. [[CrossRef](#)]

44. Sun, Y.; Zhang, M.; Mujumdar, A.S.; Yu, D. Pulse-spouted microwave freeze drying of raspberry: Control of moisture using ANN model aided by LF-NMR. *J. Food Eng.* **2021**, *292*, 110354. [[CrossRef](#)]
45. Sun, Y.; Zhang, M.; Bhandari, B.; Yang, P. Intelligent detection of flavor changes in ginger during microwave vacuum drying based on LF-NMR. *Food Res. Int.* **2019**, *119*, 417–425. [[CrossRef](#)]
46. Chen, Y.; Dong, H.; Li, J.; Guo, L.; Wang, X. Evaluation of a Nondestructive NMR and MRI Method for Monitoring the Drying Process of *Gastrodia elata* Blume. *Molecules* **2019**, *24*, 236. [[CrossRef](#)]
47. Shang, J.; Zhang, Q.; Wang, T.; Xu, Y.; Zang, Z.; Wan, F.; Yue, Y.; Huang, X. Effect of Ultrasonic Pretreatment on the Far-Infrared Drying Process and Quality Characteristics of Licorice. *Foods* **2023**, *12*, 2414. [[CrossRef](#)]
48. Malvandi, A.; Nicole Coleman, D.; Loor, J.J.; Feng, H. A novel sub-pilot-scale direct-contact ultrasonic dehydration technology for sustainable production of distillers dried grains (DDG). *Ultrason. Sonochem.* **2022**, *85*, 105982. [[CrossRef](#)]
49. Wu, X.-f.; Zhang, M.; Ye, Y.; Yu, D. Influence of ultrasonic pretreatments on drying kinetics and quality attributes of sweet potato slices in infrared freeze drying (IRFD). *Lwt* **2020**, *131*, 109801. [[CrossRef](#)]
50. Wang, J.; Xiao, H.-W.; Ye, J.-H.; Wang, J.; Raghavan, V. Ultrasound Pretreatment to Enhance Drying Kinetics of Kiwifruit (*Actinidia deliciosa*) Slices: Pros and Cons. *Food Bioprocess Technol.* **2019**, *12*, 865–876. [[CrossRef](#)]
51. Karlović, S.; Dujmić, F.; Brnčić, S.R.; Sabolović, M.B.; Ninčević Grassino, A.; Škegro, M.; Šimić, M.A.; Brnčić, M. Mathematical Modeling and Optimization of Ultrasonic Pre-Treatment for Drying of Pumpkin (*Cucurbita moschata*). *Processes* **2023**, *11*, 469. [[CrossRef](#)]
52. Walawalkar, A.K.; Poosarla, V.G.; Shivshetty, N. Impact of ultrasonication and blanching as a pre-treatment on quality parameter of dried and rehydrated bitter gourd. *Food Sci. Technol. Int.* **2023**, 10820132231177324. [[CrossRef](#)] [[PubMed](#)]
53. Wang, T.; Ying, X.; Zhang, Q.; Xu, Y.; Jiang, C.; Shang, J.; Zang, Z.; Wan, F.; Huang, X. Evaluation of the Effect of Ultrasonic Pretreatment on the Drying Kinetics and Quality Characteristics of Codonopsis & pilosula Slices Based on the Grey Correlation Method. *Molecules* **2023**, *28*, 5596. [[PubMed](#)]
54. Liu, S.; Dong, H.; Ji, W.; Zhang, M.; Duan, W.; Wang, X. Change in physicochemical properties, aroma components, and potentially beneficial compounds during the stir-frying of Massa Medicata Fermentata. *Food Chem. Adv.* **2023**, *3*, 100340. [[CrossRef](#)]

Disclaimer/Publisher’s Note: The statements, opinions and data contained in all publications are solely those of the individual author(s) and contributor(s) and not of MDPI and/or the editor(s). MDPI and/or the editor(s) disclaim responsibility for any injury to people or property resulting from any ideas, methods, instructions or products referred to in the content.